

Reactivating the extracellular matrix synthesis of sulfated glycosaminoglycans and proteoglycans to improve the human skin aspect and its mechanical properties

Hanane Chajra¹
Daniel Auriol¹
Francine Joly²
Aurélie Pagnon³
Magda Rodrigues⁴
Sophie Allart⁴
Gérard Redziniak⁵
Fabrice Lefevre¹

¹Libragen, Induchem (Givaudan Active Beauty), Toulouse, ²Sephra Pharma, Puteaux, ³Novotec, Bron, ⁴Centre de Physiopathologie de Toulouse-Purpan, Toulouse, ⁵Cosmetic Inventions, Antony, France

Background: The aim of this study was to demonstrate that a defined cosmetic composition is able to induce an increase in the production of sulfated glycosaminoglycans (sGAGs) and/or proteoglycans and finally to demonstrate that the composition, through its combined action of enzyme production and synthesis of macromolecules, modulates organization and skin surface aspect with a benefit in antiaging applications.

Materials and methods: Gene expression was studied by quantitative reverse transcription polymerase chain reaction using normal human dermal fibroblasts isolated from a 45-year-old donor skin dermis. De novo synthesis of sGAGs and proteoglycans was determined using Blyscan™ assay and/or immunohistochemical techniques. These studies were performed on normal human dermal fibroblasts (41- and 62-year-old donors) and on human skin explants. Dermis organization was studied either ex vivo on skin explants using bi-photon microscopy and transmission electron microscopy or directly in vivo on human volunteers by ultrasound technique. Skin surface modification was investigated in vivo using silicone replicas coupled with macrophotography, and the mechanical properties of the skin were studied using Cutometer.

Results: It was first shown that mRNA expression of several genes involved in the synthesis pathway of sGAG was stimulated. An increase in the de novo synthesis of sGAGs was shown at the cellular level despite the age of cells, and this phenomenon was clearly related to the previously observed stimulation of mRNA expression of genes. An increase in the expression of the corresponding core protein of decorin, perlecan, and versican and a stimulation of their respective sGAGs, such as chondroitin sulfate and heparan sulfate, were found on skin explants. The biosynthesis of macromolecules seems to be correlated at the microscopic level to a better organization and quality of the dermis, with collagen fibrils having homogenous diameters. The dermis seems to be compacted as observed on images obtained by two-photon microscopy and ultrasound imaging. At the macroscopic level, this dermis organization shows a smoothed profile similar to a younger skin, with improved mechanical properties such as firmness.

Conclusion: The obtained results demonstrate that the defined cosmetic composition induces the synthesis of sGAGs and proteoglycans, which contributes to the overall dermal reorganization. This activity in the dermis in turn impacts the surface and mechanical properties of the skin.

Keywords: cosmetic composition, decorin, dermis, polysaccharide

Correspondence: Hanane Chajra
Libragen, Induchem (part of Givaudan Active Beauty), 3 Rue des Satellites 31400 Toulouse, France
Email Hanane.chajra@givaudan.com

Introduction

Glycosaminoglycans (GAGs) are highly charged polysaccharides consisting of repeating 1→3- and/or 1→4-linked hexosamine and uronic acid residues. GAGs are

polydisperse mixtures of polysaccharide chains of varying lengths with an average molecular weight of 10^4 – 10^6 Da. Among the proteoglycans, decorin and versican are the most abundant proteoglycans in human skin.¹ Decorin is a chondroitin sulfate/dermatan sulfate proteoglycan found in the dermis in association with type I collagen, whereas perlecan, a heparan sulfate proteoglycan, is found in the basement membrane.^{2,3}

Perlecan gets a stabilizing function for basement membrane,⁴ by its interaction with type IV collagen and nidogen 1 and 2, but seems to be important also for wound healing at the functional level by the control of signaling molecules^{5,6} and stem cell niche.⁷

Decorin organizes collagen fibrils into compact fibers,⁸ and the GAG chain of decorin is involved in the control of the diameter of collagen fibrils.⁹ Versican, a chondroitin sulfate proteoglycan¹⁰ and a member of the group of aggregating proteoglycans, is localized in the basal cell layer of the epidermis, the hair follicle and sweat glands; it is in association with the elastic fibers in the dermis.^{11,12}

Versican is abundant in the dermis in comparison to the epidermis. Versican gets a hyaluronic acid binding domain at the NH₂-terminal end of the core protein. In the C-terminal region of versican, a lectin domain is identified as able to link covalently with fibrillin microfibrils,¹³ and these microfibrils are associated with elastic fibers, confirming the crucial role of versican in skin elasticity.

Although collagen type I¹⁴ is known to be the major dermis protein contributing to the mechanical properties of the skin, other molecules such as elastic fibers and proteoglycans also contribute to the overall mechanical properties of the skin.^{10,15,16} Elastic fibers are involved in the low-strain mechanical response and proteoglycans in resisting tissue compressive forces.¹⁶ The mechanical properties of the skin are also modulated by the geometric arrangement of the fibrous components.¹⁶ During aging, the mechanical properties of the skin become weak, because of the elastic network disruption,¹⁷ suggesting that the spatial assembly of the elastin and collagen networks as well as their mutual interactions dominate the dynamic mechanical response of the skin. The spatial assembly of elastic fibers and collagen fibers is also dependent on proteoglycans.¹⁶

As the stability and synthesis of GAGs and proteoglycans found in skin are known to be sensitive to ultraviolet (UV),¹⁸ aging,¹⁹ and pathologies,²⁰ a major challenge is to find a solution enabling to specifically reactivate the synthesis of these macromolecules to promote the spatial assembly of collagen and elastic fibers in a fashion similar to that observed in young skin.

Based on the known metabolic pathway of sulfated GAGs (sGAGs) and their respective proteoglycans, we designed a specific combination of biological precursors expected to stimulate skin cells to produce de novo sGAGs and their proteoglycans. In this article, we present the investigations we have conducted on this cosmetic composition to demonstrate its effects on de novo synthesis of sGAGs, especially chondroitin sulfate and heparan sulfate and of three proteoglycans important in skin physiology and structure, namely decorin, versican, and perlecan. To evaluate its efficacy as a precursor of the synthesis of sGAGs, GAG assays using Blyscan™ kit were performed. Then, to understand the mechanism of action, a gene expression analysis using quantitative reverse transcription polymerase chain reaction (qRT-PCR) was performed. The molecular synthesis of proteoglycans was followed by immunohistochemical studies.

Materials and methods

Composition developed as sGAG precursors

The composition (TIGHTENYL) has been designed based on previous results showing the effect of *N*-acetylglucosamine (GlcNAc)-6-phosphate on non-sGAG synthesis (patent US20130012475) and contains a combination of *N*-acetyl-D-glucosamine-6-phosphate, D-glucuronic acid and a magnesium sulfate in the proportions of 50–75, 55–83, and 33–66 mmol/kg, respectively. *N*-Acetyl-D-glucosamine-6-phosphate was internally produced using a proprietary technology as described in US20130012475, and all other products were purchased from Sigma-Aldrich (Saint-Quentin-Fallavier, France). The rationale behind the choice of blending glucuronic acid and magnesium sulfate with the *N*-acetyl-D-glucosamine-6-phosphate was based on the fact that these molecules are precursors (glucuronic acid) or equivalent precursors (magnesium sulfate) and (*N*-acetyl-D-glucosamine-6-phosphate) required for the synthesis of sGAGs. This composition is the mother solution and considered to be at 100%. For the various tests, this composition was assessed after dilution at various concentrations.

Gene expression studies on normal human dermal fibroblasts

45-year-old dermal fibroblasts (ref CC-2511 batch 0000477954) were purchased from Lonza (Braine-l'Alleud, Belgium). The composition at 0.5 and 1 mM (each constituent at a concentration close to 0.5 and 1 mM, respectively, due to the proper dilution of the composition in the cell

culture media) was applied on fibroblasts for 18 hours (in triplicate). Transforming growth factor- β 1 at 20 ng/mL was used as positive control. The extraction of the total RNAs was performed using the RNeasy Mini Kit (Ref. 74106) from Qiagen (Hilden, Germany). After treatment, total RNAs were extracted and their integrity was analyzed by capillary electrophoresis. For specific genes targeting the synthesis pathway of sGAGs, gene expression levels were quantified by qRT-PCR using TaqMan[®] cards from Applied Biosystems (Carlsbad, CA, USA). Normalization method used was based on the reference to a housekeeping gene, ie, glyceraldehyde-3-phosphate dehydrogenase (assay ID Hs02758991_g1). DataAssist Software v3.01 was used for data analysis. DataAssist[™] Software is a simple, yet powerful data analysis tool for sample comparison when using the comparative CT ($\Delta\Delta$ CT) method for calculating relative quantitation of gene expression.²¹ It contains a filtering procedure for outlier removal, various normalization methods based on single or multiple genes, and provides relative quantification analysis of gene expression through a combination of statistical analysis and interactive visualization. The license for using this software is limited to data generated from Applied Biosystems[®] RT-PCR instrumentation. A two-sample, two-tailed Student's *t*-test comparing the Δ CT values of the two groups is performed, and a *p*-value was calculated as both groups have more than two samples (*n*=3).

sGAG assay studies on normal human dermal fibroblasts

Normal human dermal fibroblasts were isolated from the skin dermis of 41- and 62-year-old women donors (plastic surgery). The cells were treated with the composition at 0.5 and 1 mM (each constituent at a concentration close to 0.5 and 1.0 mM, respectively) in non-supplemented medium (without fetal bovine serum) for 72 hours and incubated at 37°C in the presence of 5% CO₂. The sGAGs were then dosed in supernatants and cell pellets using Blyscan[™] assay (Kit B1000; Biocolor Ltd, Carrickfergus, UK). The dye label used in the assay was 1,9-dimethylmethylene blue (DMMB), and the dye was employed under conditions that provide a specific labeling of the sulfated polysaccharide component of proteoglycans or the protein-free sGAG chains. Total proteins were dosed in cell pellets using bicinchoninic acid assay (Sigma-Aldrich, B9643), and sGAG dosages were reported as a proportion of total amount of proteins. Each composition concentration was tested in duplicate.

Skin explants: culture and treatments

Human living skin explants were obtained from BIO-EC (Longjumeau, France) from an abdominoplasty of a 41-year-old Caucasian woman with a type II Fitzpatrick skin. After the removal of hypodermis, circular skin explants were excised using a biopsy punch instrument. The explants were placed at the air–liquid interface in BIO-EC's Explant Medium (BEM[®]) and cultured under classical cell culture conditions (37°C in 5% CO₂).

The composition was diluted in water at 0.5 mM and topically applied on normal human skin explants kept in survival on day 0, day 1, day 2, day 5, day 6, day 7 and day 8. The control explants did not receive any treatment except the renewal of the medium. Each condition was studied in triplicate. Each explant was cut into four parts. The first quarter was fixed in buffered formalin, and the second quarter was frozen at -80°C for immunohistological analyses. The third quarter was fixed in 0.1 M cacodylate buffer pH 7.35 containing 2% glutaraldehyde during 24 hours at 4°C; it was then rinsed with 0.2 M cacodylate buffer and stored at 4°C until inclusion for transmission electron microscopy observations. The fourth quarter was fixed in 3% paraformaldehyde diluted in 0.1 M phosphate-buffered saline (PBS; pH 7.4) (Sigma-Aldrich, Ref. P-3813) during 2 hours at 4°C, then rinsed in PBS and stored at 4°C for two-photon analyses.

sGAG and proteoglycan visualization (immunostaining) and quantification (image analysis) on human skin explants

Immunostainings

Heparan sulfate immunostaining was realized on 5–7 μ m-thick frozen sections with an anti-heparan sulfate monoclonal antibody (clone A7L6; Ref. MA1-06821; Thermo Fisher Scientific, Waltham, MA, USA), diluted at 1:100 with water and revealed by fluorescein isothiocyanate (SA 1001; Invitrogen, Waltham, MA, USA). Chondroitin sulfate immunostaining was realized on 5–7 μ m-thick paraffinized sections with an anti-chondroitin sulfate monoclonal antibody (clone CS-56; Ref. ab11570; Abcam), diluted at 1:400 with water and revealed by Vector[®] VIP peroxidase substrate (Ref. SK-4600; Vector Laboratories, Burlingame, CA, USA). Decorin immunostaining was realized on frozen sections with an anti-decorin monoclonal antibody (clone 9XX, Ref. sc-73896; Santa Cruz Biotechnology, Santa Cruz, CA, USA), diluted at 1:200 with water. Nuclei were post-stained with propidium iodide. The immunostainings were assessed by microscopic observations.

Image analysis

The percentage of area occupied by the stained target in the area of interest is measured for each image using the CellID software (Olympus).

The percentage of surface was calculated according to the surface of the region of interest and the surface of the staining selected by threshold. For the image analysis of chondroitin sulfate and heparan sulfate, the region of interest is a band of 15 μm below the dermo-epidermal junction (DEJ) in the papillary dermis. For the image analysis of decorin, the region of interest is the dermis area. For each batch, 9–12 images are analyzed. For each image analysis, the threshold is defined and used for all the images, only the region of interest is drawn for each image.

Statistical analysis

To define if the difference between two results of image analysis is significant, we calculated the probability p . The probability p was determined by the Student's t -test (two-tailed, different variance) using the PRISM 5.04 software (GraphPad Software). If p is <0.05 , there is a probability of 95% for the two results to be significantly different.

Telocytes visualization (double immunostaining) and quantification (image analysis) on human skin explants

Telocytes are known to express two markers CD34 (also known as human hematopoietic progenitor cell antigen) and platelet-derived growth factor receptor (PDGFR) α .²² The double immunostaining of telocytes has been realized on paraffinized sections using a monoclonal anti-CD34 antibody (Ref. sc-19587; Santa Cruz Biotechnology) and a polyclonal anti-PDGFR- α antibody (Ref. PA5-32545; Thermo Fisher Scientific). Both antibodies have been diluted 1/50 in PBS–bovine serum albumin (0.3%). The histological slides were incubated first with an anti-PDGFR- α antibody during 1 hour at room temperature and revealed by VIP (violet staining, Ref. SK-4600; Vector Laboratories). Successively, the slides were incubated overnight at room temperature with the antibody anti-CD34 and revealed by SG (blue staining, Ref. SK-4700; Vector Laboratories).

Image analysis

For each batch (15 images), the number of positive cells (CD34+, PDGFR α + and CD34+/PDGFR α +) have been counted and reported to the total amount of positive cells to obtain the percentage of positive cells/100 positive

cells/ mm^2 in the papillary dermis. The surface of papillary dermis has been measured using the CellID Olympus software.

Dermis reorganization studies using transmission electron microscopy and two-photon microscopy on human skin explants

The dermis organization of skin explants treated with the composition was assessed by bi-photon microscopy. Skin explants after 8 days of culture and 2 hours of fixation with 3% paraformaldehyde were rinsed in PBS and embedded in optimal cutting temperature and frozen at -70°C , then 50- μm -thick frozen sections were performed in sagittal position allowing the observation of all skin strata. Images were obtained with an AxioImager upright microscope LSM Carl Zeiss 7MP (Carl Zeiss, Jena, Germany). A pulsed femtosecond Ti:sapphire laser (Chameleon Ultra II; Coherent Inc, Santa Clara, CA, USA) tunable in the range of 690–1064 nm was used as the excitation light source. Emitted light is detected through a descanned pathway leading to five non-descanned detectors. Tile scan images were acquired to cover the entire skin slice, in 512×512 pixel dimensions for each scan, with an immersion 20 \times objective. Then, 47 μm z-stacks were acquired, with a sampling of 0.78 μm . The laser was set to deliver the wavelength at 940 nm. Second harmonic generation (SHG) signal for collagen was detected in reflection (backward SHG) using a cube with a 485 nm short-pass filter. Green autofluorescence emission corresponding to elastic fibers was detected using a filter cube with 500–550 nm band-pass filter. The dermis ultrastructure was also assessed by transmission electron microscopy with a focus on collagen fibers, elastic fibers and telocytes (a cell type described as important in skin homeostasis and regeneration process) structures. After sample fixation in 2% glutaraldehyde in 0.1 M cacodylate buffer followed by rinsing with 0.2 M pH7.35 cacodylate buffer, a postfixation was performed with 1% osmium tetroxide solution in 0.1 M cacodylate buffer. Then, the samples were washed very quickly in distilled water and were dehydrated through a graded series of ethanol baths (from 30% to 100% for 15 minutes at room temperature). The resin infiltration was performed with a mix of 100% ethanol–epoxy resin, then with epoxy resin + 1.7% benzyltrimethylamine (BDMA) resin for 1 hour at room temperature. Samples were embedded in fresh resin (epon + 1.7% BDMA) in tagged molds, and the polymerization was performed for 72 hours at 56°C . For transmission electron microscope analysis, ultra-thin 50 nm

sections were stained with uranyl acetate and lead citrate and observed with a Philips CM120 electron microscope (Centre Technologique des Microstructures, Université Lyon 1, France) equipped with a Gatan Orius 200 2K×2K digital numeric camera (Gatan, Abingdon, UK).

Clinical study design

A total of 24 female participants in the age range of 47–65 years participated in the study, 50% of them being menopausal. All subjects gave their written informed consent. The recommendations of the Declaration of Helsinki and the guidelines of the InterConference on Harmonization of Good Clinical Practice were observed as applicable to a non-drug study. In France according to Directive 2001/20/EC initiated with the issue of Law No. 2004-806 in August 2004 (relating to the public health policy), followed by Decree No. 2006-477, which was published on April 26, 2006, and article L1121-1 related to the definition of specific biomedical researches, for noninterventional cosmetic studies on humans, it's not mandatory to request the approval from an IRB or ethical committee.

The efficacy of the composition formulated in a cream containing the following components aqua, octyldodecyl neopentanoate, octyldodecanol, myristyl myristate, phenoxyethanol, carbomer, acrylates/C10-30 alkyl acrylate crosspolymer, sodium hydroxide, methylparaben, perfume, butylparaben, ethylparaben, propylparaben with 2% of the defined composition (0.5 mM) was evaluated in a double-blind test vs placebo under dermatological control. The participants applied twice a day the placebo on one side of their face, and twice a day a cream containing 2% of the composition on the other side.

The assessments of skin echogenicity (ultrasound tool) and skin surface (silicone replicas) were performed after 84 days of product application. The effect of the composition on skin dermis organization was evaluated by ultrasound equipment. Skin echogenicity was measured directly on maxillaries, using the high-frequency echograph DermaScan C[®] 2D (Cortex Technology, Hadsund, Denmark). The ultrasound used had a 20 MHz probe. This method allowed the visualization of the skin, on the epidermis and dermis levels, with a 13 mm penetration. During the picture acquisition, the conjunctive tissue, echogenic, appears in color (from yellow to green); non-echogenic tissues appear in black. Silicone replicas were made to visualize the skin surface to illustrate the benefit of the product for the volunteer. The determination of the mechanical property of the skin (firmness) was performed after 14 days of product application with an MPA 580 Cutometer[®] (Courage & Khazaka) connected to a computer.²³

These measurements define different the parameters such as Uf (final distention) and Uv (delayed distension) characterizing, respectively, the skin firmness and plasticity, the two mechanical properties of the skin.²⁴ In this study, we focused on skin firmness and skin plasticity. The technique consists in skin suction by a measurement probe by constant vacuum pressure for a set length of time. The depth to which the skin penetrates into the probe is measured by two optical prisms located at the opening of the probe's orifice to eliminate the effects of friction and mechanical strain. Measurements of skin firmness (Uf) and skin plasticity (Uv) were performed with a 2 mm probe, with a constant pressure of 450 mbar. The time of suction and relaxation is of 3 seconds. Three consecutive cycles are made. Each measurement is an average of two acquisitions in close zones. Skin firmness was determined by the parameter Uf, and skin plasticity was determined by the parameter Uv calculated by Uf-Ue. Ue means immediate skin distension. A decrease in UF parameter characterizes a tensing effect with a firmer skin. A decrease in UV parameter characterizes an improvement of skin plasticity associated with a younger behaving skin. Data analysis for each parameter was conducted by descriptive statistics (mean, standard deviation) using Microsoft[®] excel 2010 and SAS v9.4. Then, for inferential analysis, a mixed ANOVA for repeated measures (Proc Mixed), including the factors product and time as fixed, and subject as random, was fitted on raw data. From this model, the within-product comparisons and the between-product comparisons were performed, in terms of change from baseline using the estimated means. The type I error was set at $\alpha=0.05$ in bilateral approach.

Results and discussion

Modulation of enzymes involved in the synthesis pathway of sGAG leading to effective synthesis of these macromolecules

The synthesis of the polysaccharide side chain of the sulfated proteoglycans such as heparan sulfate, chondroitin sulfate, and dermatan sulfate as well as their sulfate decoration is a process with three distinct steps that requires the action of specialized enzymes.²⁵ The first enzymes involved are specialized transferases that are able to initiate the polysaccharide chain formation through the synthesis of a linker oligosaccharide attached to a serine residue present in the core protein. It must be underlined that they play a crucial role in obtaining homogenous oligosaccharide linkers. The second type of enzymes is GAG synthases that transfer uridine 5'-diphosphate (UDP)-monosaccharides to acceptor

oligosaccharide, and finally GAG sulfotransferases introduce a sulfo group to the appropriate position on the polysaccharide backbone. Remarkably, the defined composition induces overexpression of several genes involved in the three stages of this process (initiation, modification, and elongation; Figure 1). An effect was seen at initiation stage by the modulation of galactosyltransferase I (B4GALT7) gene expression. This enzyme catalyzes the transfer of a galactose residue from UDP-galactose donor substrate onto the hydroxyl of the xylose linked to serine residue on the core protein. In addition, at the initiation stage, glucuronosyltransferase I (B3GAT3) allows the transfer of a glucuronyl residue during the final synthesis reaction of the linker tetrasaccharide. Once the formation of the tetrasaccharide linker has been achieved, the elongation stage of sGAG chains begins. The nature of the first saccharide residue transferred on the primer tetrasaccharide determines the type of GAGs chains synthesized: the addition of *N*-acetylgalactosamine will direct the cellular machinery toward the synthesis of chondroitin sulfate/dermatan sulfate chains, whereas the addition of GlcNAc will direct the cellular machinery toward the synthesis of heparan sulfate. The extension of the chains is possible through the addition of two monosaccharides alternatively, hexosamine and glucuronic acid. These reactions are catalyzed by heparan sulfate and chondroitin sulfate synthases.

The synthesis of heparan sulfate chains is associated with the expression of exostosin glycosyltransferase (EXT) genes family. The exostosin-like glycosyltransferase (EXTL2) initiates the chain elongation phase via the transfer of the first GlcNAc residue to the tetrasaccharide linker of the core protein. EXTL2 is an essential enzyme for the regulation of the synthesis of heparan sulfate.²⁶ This reaction is followed by the sequential addition of glucuronic acid and GlcNAc residues catalyzed by a complex formed with EXT1 and EXTL2. The EXT1 has two catalytic activities, one glucuronyl acid transferase and one *N*-acetylglucosaminyltransferase allowing for the alternative addition of glucuronic acid and GlcNAc on the tetrasaccharide linker attached to the core protein.

The synthesis of chondroitin sulfate and dermatan sulfate chain occurs through the action of chondroitin sulfate synthase 1 (CHSY1), which adds alternatively glucuronic acid and *N*-acetylgalactosamine residues. Glucuronic acid from chondroitin sulfate chains undergoes epimerization to form iduronic acid residues through the activity of dermatan sulfate epimerase; the resulting GAG is then dermatan sulfate. Concerning the chain modifications, an overexpression of *N*-acetylgalactosamine sulfotransferases such as carbohydrate chondroitin 4 sulfotransferase 12 (CHST12) and carbohydrate *N*-acetylgalactosamine 4-sulfate 6-O sulfotransferase 15 (CHST15) was observed with the composition.

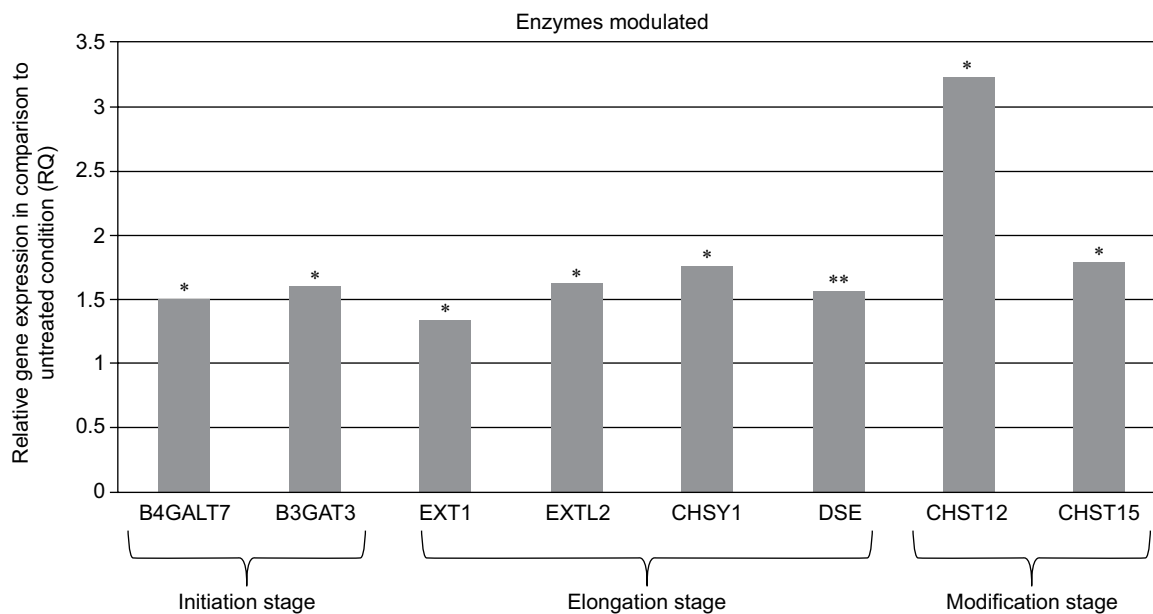


Figure 1 Modulation of mRNA expression of enzymes after fibroblast treatment with the composition.

Notes: RQ is the relative gene expression in comparison to untreated cells (RQ > 1: increased gene expression and the statistical significance is represented by * for *p*-values < 0.05 and ** for *p*-values < 0.01).

Abbreviations: B3GAT3, beta-1,3-glucuronyltransferase 3 (glucuronosyltransferase I); B4GALT7, xylosylprotein beta 1,4-galactosyltransferase, polypeptide 7; CHST12, carbohydrate chondroitin 4 sulfotransferase 12; CHST15, carbohydrate *N*-acetylgalactosamine 4-sulfate 6-O sulfotransferase 15; CHSY1, chondroitin sulfate synthase 1; DSE, dermatan sulfate epimerase; EXT1, exostosin glycosyltransferase 1; EXTL2, exostosin-like glycosyltransferase.

Results shown in Figure 1 show that when using the composition, the relative gene expressions are increased by ~50% except for CHST12; independently of the exact values of increases, the important observation is that these overexpressions concern several genes involved in the synthesis of sGAGs. It can thus be assumed that the composition has a positive effect on the global accumulation of GAGs. Since increase of mRNA expression of enzymes involved in sGAGs synthesis does not mean necessarily an increase in GAGs production, we quantified also the sGAGs production. sGAGs were detected using DMMB assay and antibodies.^{27,28} Indeed, DMMB is widely used to quantify sGAG contents in engineered tissues, whereas antibodies are used to discriminate and visualize (tissular location) specific sGAGs such as heparan sulfate and chondroitin sulfate. Figures 2 and 3 show that the defined formulation increases the content of sGAGs (heparan sulfate and chondroitin sulfate) when considering the control as reference in cell cultures or skin explants maintained in survival.

Impact of the modulation of sGAG synthesis on dermis structure and mechanical properties and surface of the skin

Skin ultrasound examinations are often used in the medical field to evaluate healthy and pathologically altered skin.²⁹ In the current study, we used this technique to monitor the change that takes place in an aged skin and especially in the dermis following the de novo synthesis of sGAGs (Figure 4B). Figure 4B shows that papillary and reticular dermis of a 47-year-old donor skin is loose (characteristic of aged skin) with huge non-echogenic areas (black areas), but once treated with the composition twice a day for 84 days, the skin is compacted with significantly less non-echogenic areas. This observation is consistent with bi-photon images (Figure 4) showing a fibrillar and homogenous dermis in comparison to untreated skin condition. The dermis structure of an aged skin characterized by collagen bundles appearing to be unravel is shown in Figure 4A.³⁰ Interestingly, the role of decorin components, core protein and sGAG chains, in collagen protection and collagen arrangement, was described by several authors.^{9,31,32} Indeed, collagen disorganization and degradation was found in tissues having either truncated decorin core protein (as a consequence of UV irradiation³² or genetic disorders³¹) or altered sGAG chains (in aged skin).^{33,34} It has been shown that the level of mRNA expression of decorin is also impacted by aging and by UV irradiation.³⁵ In our study, we have shown that the composition once topically

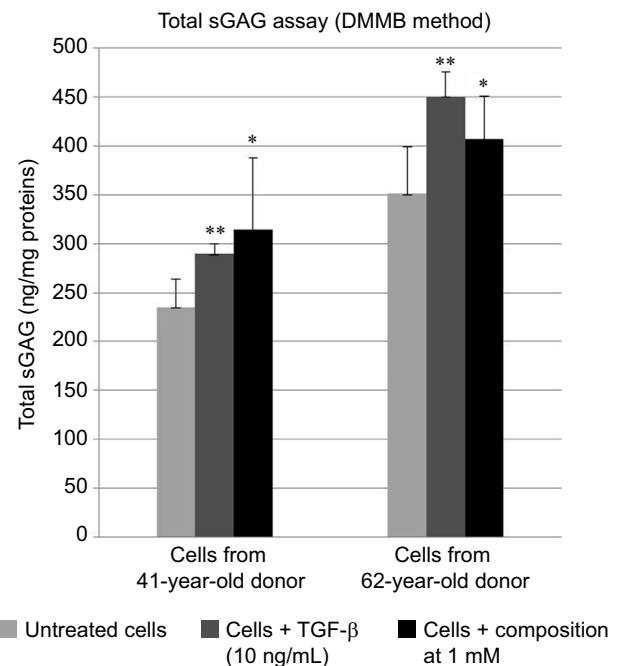


Figure 2 sGAGs detected by DMMB assay and immunostainings using specific antibodies for chondroitin sulfate and heparan sulfate.

Notes: A significant increase in the total sGAGs was obtained for both cell types: this suggests that the composition acts not only by an effect on protein expression but also by an increase in the synthesis of chondroitin sulfate and heparan sulfate demonstrating the effect of the composition. An overexpression for chondroitin sulfate and heparan sulfate was demonstrated in skin tissue sections, treated with the composition. The quantification of chondroitin sulfate and heparan sulfate expressions were performed using image analysis. A nonsignificant increase by +14% of the chondroitin sulfate expression and a significant increase in heparan sulfate by +13.8% were determined. The statistical significance was determined using Student's t-test and represented by * for p -values <0.05, and ** for p -values <0.01.

Abbreviations: DMMB, 1,9-dimethylmethylen blue; sGAGs, sulfated glycosaminoglycans; TGF, transforming growth factor.

applied on a 41-year-old skin explant was able to stimulate both decorin component expression such as core protein (Figure 5) and chondroitin sulfate (Figure 3A). These results confirmed that decorin is able to organize the collagen structure of an aged and disorganized tissue (Figure 4A). Moreover, by transmission electron microscopy, we observed, in these explants (Figure 6), that the diameter of collagen fibrils seems to be more homogenous in treated skin in comparison to untreated skin condition (Figure 6D, black box). We have also noticed in skin explants treated with the composition higher amount of versican and perlecan in comparison to untreated skin explants (data not shown). Collagen content quantification allowed us to conclude that this compaction is not the consequence of the collagen overexpression. Moreover, we found in vivo that the dermis compaction (Figure 4A and B) leads to an improvement in the mechanical properties of the skin (Table 1) and to a smoothing effect on the skin surface with less visible wrinkles similar to that seen after a lifting treatment (Figure 4C and Table 2). Indeed, it is known that the mechanical properties of a connective tissue (eg, dermis)³⁶

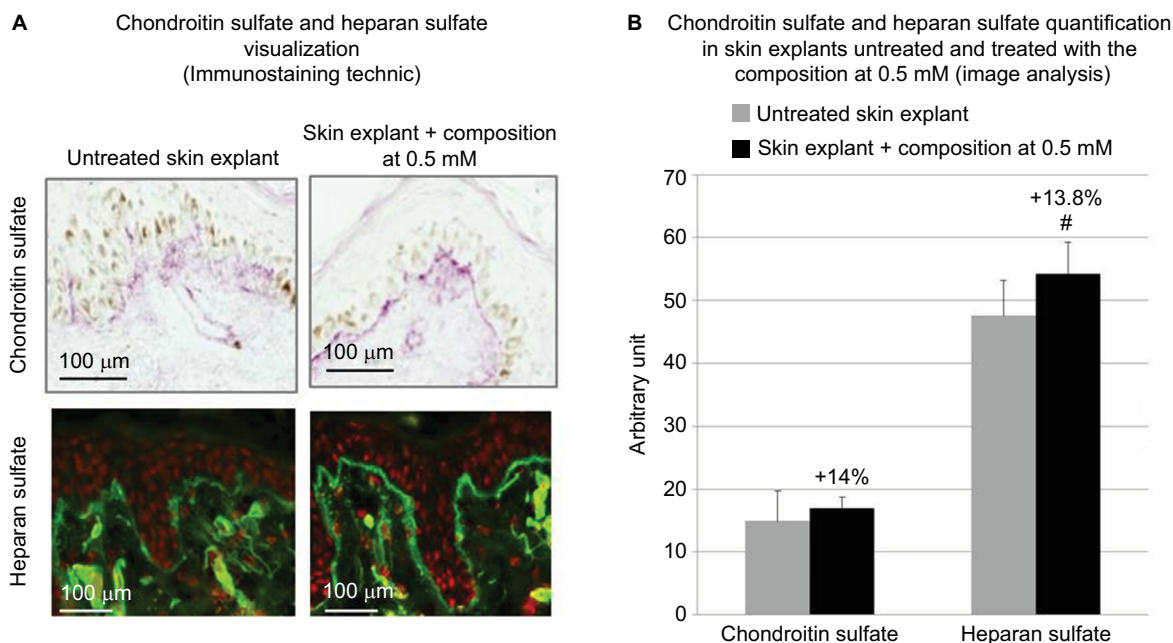


Figure 3 (A) sGAGs detected by immunostainings using specific antibodies for chondroitin sulfate and heparan sulfate. **(A and B)** An overexpression for chondroitin sulfate and heparan sulfate was demonstrated in skin tissue sections, treated with the composition. **(B)** The quantification of chondroitin sulfate and heparan sulfate expressions was performed using image analysis. A nonsignificant increase by +14% of the chondroitin sulfate expression and a significant increase in heparan sulfate by +13.8% were determined. The statistical significance was determined using Student's t-test and represented by # for p -values < 0.1 . The study was performed in triplicate with 41-year-old skin explants.

Abbreviation: sGAGs, sulfated glycosaminoglycans.

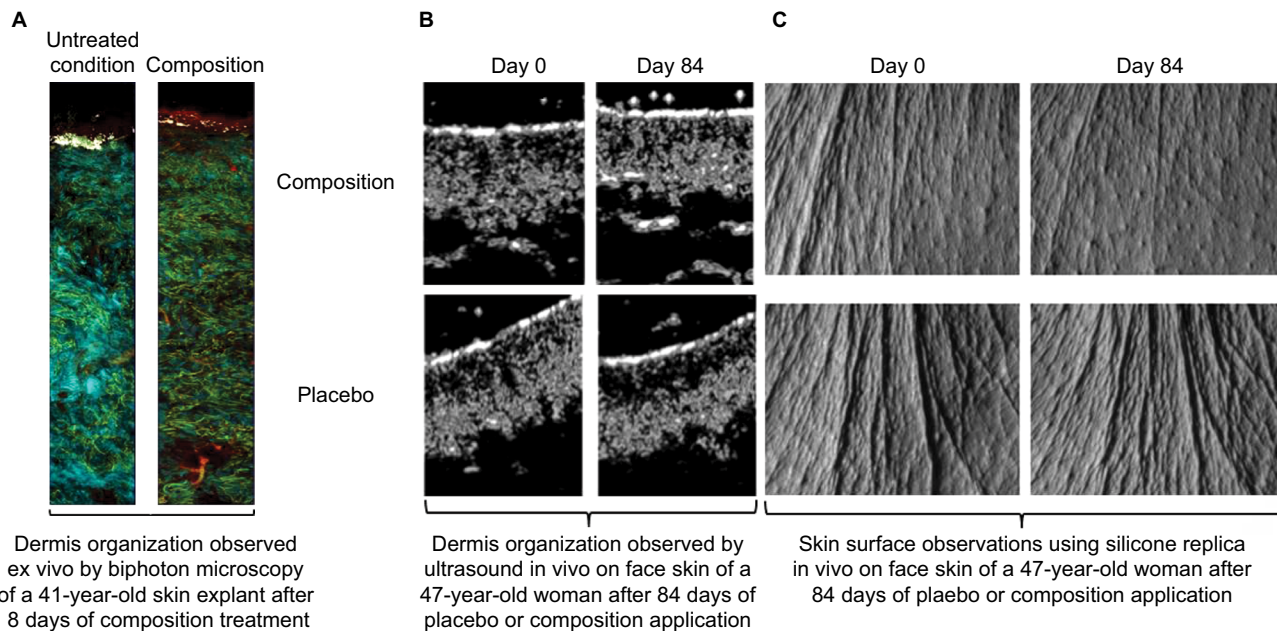


Figure 4 Modulation of dermis structure of skins treated with the composition studied either **(A)** ex vivo (41-year-old skin explants, bi-photon microscopy) or **(B and C)** in vivo (47-year-old women).

Notes: **(B)** Skin structures observed by ultrasound; **(C)** skin surfaces analyzed by silicone replica.

are linked to its three-dimensional arrangement based on three major components: collagen, elastic fibers, and proteoglycans.³⁷ In this study, we found that modulating the proteoglycan component (and specifically the dermatan sulfate chains on decorin) leads to dermis structure modification

associated with better mechanical properties (more firmness and more elasticity). Our findings are consistent with those published by Lewis et al,³⁸ showing, in neo-cartilage model, that the dermatan sulfate chains on decorin influences the organization and mechanical properties of the neo-cartilage.

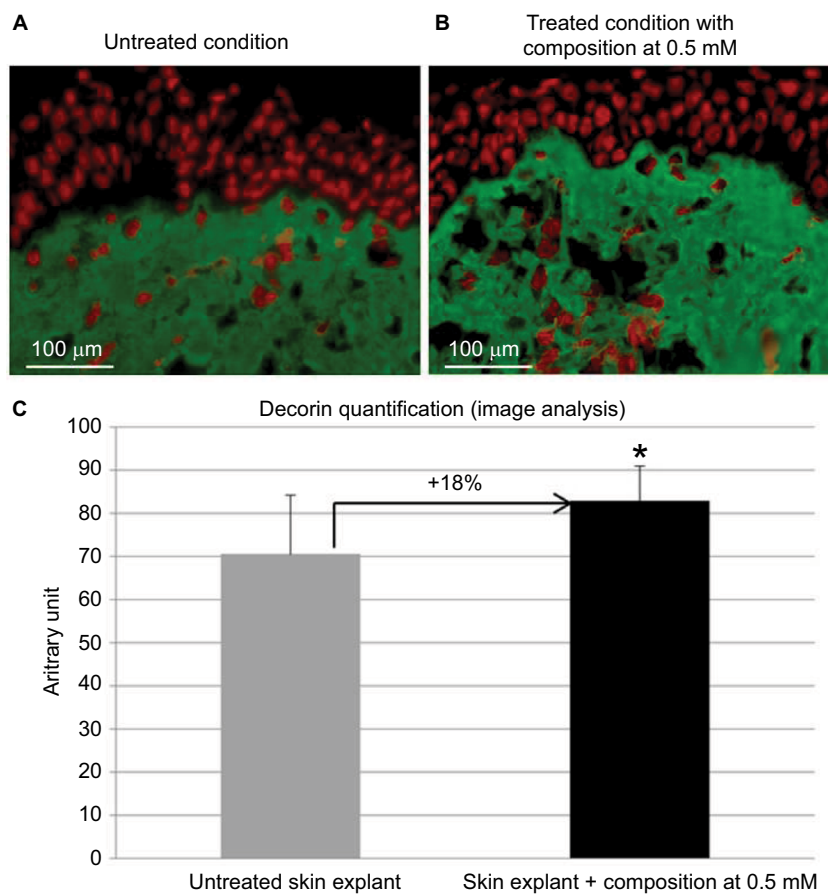


Figure 5 Visualization of core protein decorin expression in skin explants treated (B) with or (A) without cosmetic composition at 0.5 mM for 8 days and maintained in survival.

Notes: A significant increase in the expression of decorin by +18% was measured by image analysis in skin explants treated with the composition at 0.5 mM in comparison to untreated skin explants (C). The statistical significance was determined by Student's *t*-test and represented by * for *p*-values <0.05. The study was performed in triplicate with 41-year-old skin explants.

Table I Variations of biomechanical properties of the skin after 14 days of twice-daily use of a cosmetic composition at 0.5 mM in comparison to a placebo cream

Parameters	Variations of biomechanical properties of the skin after 14 days of twice-daily use in comparison to the initial state		Comparison between placebo cream and composition cream
	Human skins treated with the placebo cream: mean \pm standard deviation; percentage of improvement; statistical significance (<i>p</i> -value)	Human skins treated with cream containing the composition at 0.5 mM: mean \pm standard deviation; percentage of improvement; statistical significance (<i>p</i> -value)	
Uf parameter (firmness)	-0.024 ± 0.009 ; -8%; <i>p</i> =0.014	-0.045 ± 0.010 ; -14%; <i>p</i> <0.0001	-6%; <i>p</i> <0.05
Uv parameter (plasticity)	-0.011 ± 0.003 ; -12%; <i>p</i> <0.0001	-0.020 ± 0.003 ; -22%; <i>p</i> <0.0001	-10%; <i>p</i> =0.003

Notes: In the Cutometer analysis, 24 volunteers were enrolled. A significant improvement in skin firmness and skin plasticity was measured. Uf, final distention; Uv, delayed distension.

It must be stated that the advantage of the composition vs a lifting treatment is that the composition works without the drawbacks encountered during invasive (surgical procedure³⁹), or noninvasive lifting procedures (laser, radiofrequency and micro-focused ultrasound [MFU] devices). These techniques are not affordable and need to

be performed several times in a year because the effect obtained is not persistent. MFU was recently proposed as an alternative new safe solution for skin tightening.⁴⁰⁻⁴² MFU heats the skin at a temperature of >60°C and induces not only collagen denaturation and contraction but also de novo collagen synthesis and skin remodeling. MFU treatment is

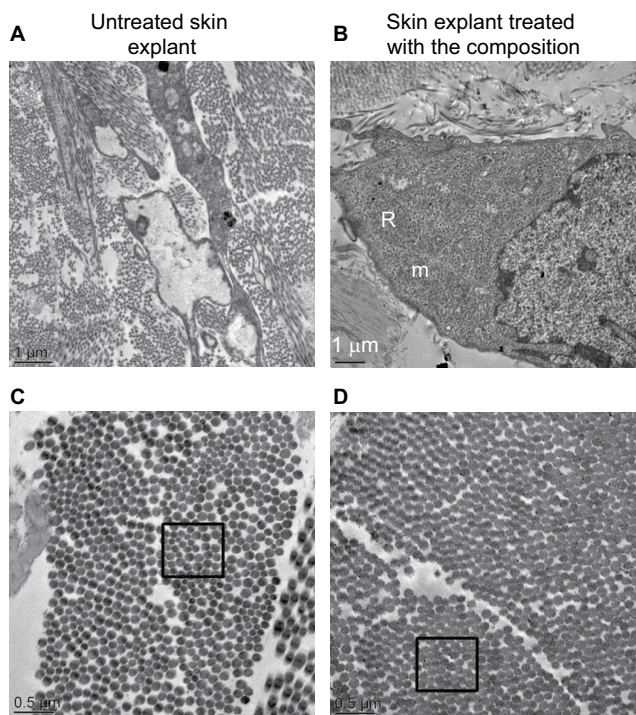


Figure 6 Observations by transmission electron microscopy of a 41 year old skin explant treated with or without the composition.

Notes: (A) Telocytes with abnormal morphology and low metabolism in untreated skin conditions. (B) Telocytes with a high metabolic activity confirmed by the presence of numerous mitochondria and granulous endoplasmic reticulum. (C) In the untreated skin explant, the diameter of collagen fibrils appears heterogenous, (D) whereas in treated skin explant the diameter of collagen fibril is homogenous (as shown before the specific black boxes in C and D).

Abbreviations: m, mitochondria; R, reticulum.

unfortunately associated with adverse events such as mild edema, moderate-to-severe prolonged erythema and mild scabbing. Although these adverse events can be resolved after 3 months without complications,⁴³ its replacement to invasive surgical procedures is impossible because its efficacy is not reliable and not persistent as a new session of MFU is required after 3 months. Then, it is advised to use oral nonsteroidal anti-inflammatory drugs to minimize the discomforts occurring

during treatment.⁴² In comparison to these drawbacks of lifting treatments, the use of a cosmetic product seems to be affordable, easy and safe solution to achieve the same result.

Incidentally, during tissue observations by transmission electron microscopy, we noticed that a recently described cell type, telocytes,⁴⁴ seems to be sensitive to the modulation of expression of sGAGs and decorin induced by the composition. Telocytes are interstitial cells found in a wide variety of mammalian organs. Their roles are not fully clear, but several authors suggest their involvement in skin homeostasis, skin remodeling, skin regeneration, and skin repair.^{22,44,45} Indeed, in untreated skin explants observed by transmission electron microscopy, the telocytes were found to be quasi-inexistent and almost dead or having an abnormal morphology (Figure 6A), but in skin explants treated with the composition (Figure 6B), these cells were numerous and metabolically active (Figure 6B). Using double immunostaining with CD34 and PDGFR alpha markers, we confirmed that the cells observed by transmission electron microscopy were really telocytes. We completed the study by their quantification confirming their statistically significant increase in the skin once treated with the composition (Figure 7). In the present case, we could assume that these cells are also involved in tissue organization by helping fibroblast activities to produce sGAGs and proteoglycans involved in tissue organization. Our assumption seems to be shared by Manetti et al,⁴⁶ as they thought that the progressive loss of telocytes might contribute to the altered three-dimensional organization of the extracellular matrix and reduce the control of fibroblasts, leading to impaired skin regeneration.

Conclusion

Our investigations demonstrated that in aged skins, the use of a cosmetic composition containing *N*-acetyl-d-glucosamine-6-phosphate, d-glucuronic acid, and magnesium sulfate

Table 2 Analysis of cutaneous microrelief from skin prints using Skin Image Analyzer® before and after 84 days of placebo or composition cream application

Parameters	Placebo			Composition			Composition cream vs placebo cream (%; p-value)
	Depth of microrelief furrows in µm (mean ± standard deviation) (arbitrary unit)	Average variation vs D0 (%; p-value)	Percentage of subjects with a smoothing effect	Depth of microrelief furrows in µm (mean ± standard deviation) (arbitrary unit)	Average variation vs D0 (%; p-value)	Percentage of subjects with a smoothing effect	
D0	32.9±0.4			33.3±0.3			
D84	33.3±0.3	+1%; p=0.348	78%	32.6±0.4	-2%; p=0.054	48%	-3%; p=0.04
Number of subjects	23			21			

Notes: Skin Image Analyzer® determines the depth of microrelief furrow in micrometer. A significant reduction in the depth of microrelief furrow was measured on 78% of subjects involved in the study and treated with the composition. The number of subjects selected and analyzed for the parameter “depth of microrelief” was 23 and 21 for placebo and composition cream group, respectively, instead of 24 because aberrant values were recorded.

Abbreviation: D, day.

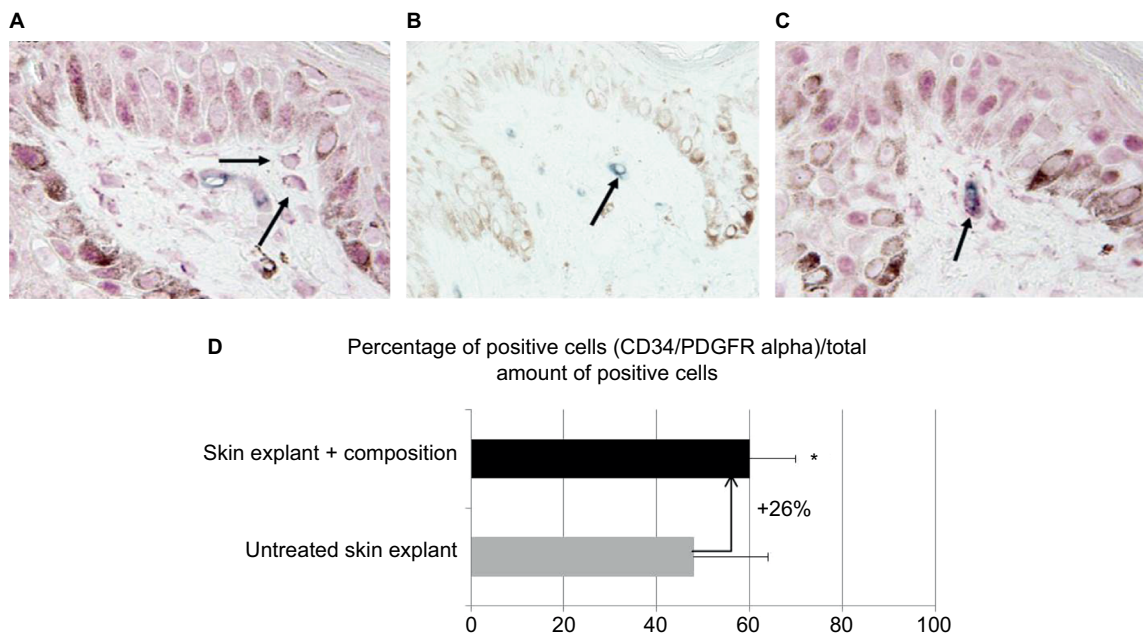


Figure 7 (A) Immunostaining of cells only positive to PDGFR alpha marker (red signal is indicated by black arrows). (B) Immunostaining of cells only positive to CD34 marker (blue signal is indicated by black arrow). (C) Immunostaining of cells positive to both markers PDGFR alpha and CD34 (superposition of red and blue signals is indicated by black arrow).

Notes: (D) A chart representative of the percentage of positive cells to both CD34 and PDGFR alpha found in skin explants treated with or without the composition. As shown in D, a statistically significant increase by 26% of the percentage of cells double marked with CD34 and PDGFR was observed in skin explants treated with the composition in comparison to untreated skin explants. The statistical significance was determined by Student's *t*-test and represented by * for *p*-values <0.05.

Abbreviation: PDGFR, platelet-derived growth factor receptor.

enables to stimulate de novo synthesis of sGAGs and proteoglycans. These new syntheses might be explained by a stimulation of the gene expression of several key enzymes involved in the three main steps of the synthesis of sGAG and proteoglycans in skin, as we have shown that their mRNA level of expression was significantly increased under the treatment of fibroblasts with the composition. Moreover, we confirmed, on aged skin explants treated with the composition, the important role of sGAGs and proteoglycans and especially decorin in the overall dermis organization as shown previously by others researchers.^{9,47} The overexpression of sGAGs and proteoglycans seen in the skin explants was associated with a better collagen fibril diameter control, appearing homogenous, packed, and unraveled. These observations were confirmed by three techniques (echography, two-photon microscopy and transmission electron microscopy). Finally, the benefits of stimulating the synthesis of sGAGs and proteoglycans were confirmed during a clinical test on human volunteers with aged skin showing at the macroscopic level that the reorganization of the dermis fibers enables a lifting effect after 3 months of treatment. The skin of the volunteers appears smoother and firmer with fewer wrinkles.

Acknowledgments

The authors would like to thank Laurent Peno-Mazzarino and Dr Elian Lati for the immunohistological studies (Laboratoire

Bio-EC, Longjumeau, France). The authors also thank Dr Michel Salmon and Dr Aline Chretien for mRNA studies (Straticell, Isnes, Belgium). This work was funded by Libragen, Induchem.

Disclosure

The authors Hanane Chajra, Fabrice Lefevre and Daniel Auriol are Libragen employees.

The authors report no other conflicts of interest in this work.

References

- Carrino DA, Calabro A, Darr AB, et al. Age-related differences in human skin proteoglycans. *Glycobiology*. 2011;21(2):257–268.
- Bianco P, Fisher LW, Young MF, Termine JD, Robey PG. Expression and localization of the two small proteoglycans biglycan and decorin in developing human skeletal and non-skeletal tissues. *J Histochem Cytochem*. 1990;38(11):1549–1563.
- Breitkreutz D, Koxholt I, Thiemann K, Nischt R. Skin basement membrane: the foundation of epidermal integrity – BM functions and diverse roles of bridging molecules nidogen and perlecan. *Biomed Res Int*. 2013;2013:179784.
- Behrens DT, Villone D, Koch M, et al. The epidermal basement membrane is a composite of separate laminin- or collagen IV-containing networks connected by aggregated perlecan, but not by nidogens. *J Biol Chem*. 2012;287(22):18700–18709.
- Patel VN, Likar KM, Zisman-Rozen S, et al. Specific heparan sulfate structures modulate FGF10-mediated submandibular gland epithelial morphogenesis and differentiation. *J Biol Chem*. 2008;283(14):9308–9317.
- Whitelock JM, Melrose J, Iozzo RV. Diverse cell signaling events modulated by perlecan. *Biochemistry*. 2008;47(43):11174–11183.

7. Dos Santos M, Michopoulou A, André-Frei V, et al. Perlecan expression influences the keratin 15-positive cell population fate in the epidermis of aging skin. *Aging (Albany NY)*. 2016;8(4):751–768.
8. Raspanti M, Viola M, Forlino A, Tenni R, Gruppi C, Tira ME. Glycosaminoglycans show a specific periodic interaction with type I collagen fibrils. *J Struct Biol*. 2008;164(1):134–139.
9. Rühlend C, Schönherr E, Robenek H, et al. The glycosaminoglycan chain of decorin plays an important role in collagen fibril formation at the early stages of fibrillogenesis. *FEBS J*. 2007;274(16):4246–4255.
10. Zimmermann DR, Dours-Zimmermann MT, Schubert M, Bruckner-Tuderman L. Versican is expressed in the proliferating zone in the epidermis and in association with the elastic network of the dermis. *J Cell Biol*. 1994;124(5):817–825.
11. du Cros DL, LeBaron RG, Couchman JR. Association of versican with dermal matrices and its potential role in hair follicle development and cycling. *J Invest Dermatol*. 1995;105(3):426–431.
12. Bode-Lesniewska B, Dours-Zimmermann MT, Odermatt BF, Briner J, Heitz PU, Zimmermann DR. Distribution of the large aggregating proteoglycan versican in adult human tissues. *J Histochem Cytochem*. 1996;44(4):303–312.
13. Isogai Z, Aspberg A, Keene DR, Ono RN, Reinhardt DP, Sakai LY. Versican interacts with fibrillin-1 and links extracellular microfibrils to other connective tissue networks. *J Biol Chem*. 2002;277(6):4565–4572.
14. Silver FH, Freeman JW, DeVore D. Viscoelastic properties of human skin and processed dermis. *Skin Res Technol*. 2001;7(1):18–23.
15. Carrino DA, Sorrell JM, Caplan AI. Age-related changes in the proteoglycans of human skin. *Arch Biochem Biophys*. 2000;373(1):91–101.
16. Silver FH, Kato YP, Ohno M, Wasserman AJ. Analysis of mammalian connective tissue: relationship between hierarchical structures and mechanical properties. *J Long Term Eff Med Implants*. 1992;2(2–3):165–198.
17. Ventre M, Mollica F, Netti PA. The effect of composition and microstructure on the viscoelastic properties of dermis. *J Biomech*. 2009;42(4):430–435.
18. Shin JE, Oh JH, Kim YK, Jung JY, Chung JH. Transcriptional regulation of proteoglycans and glycosaminoglycan chain-synthesizing glycosyltransferases by UV irradiation in cultured human dermal fibroblasts. *J Korean Med Sci*. 2011;26(3):417–424.
19. Oh JH, Kim YK, Jung JY, Shin JE, Chung JH. Changes in glycosaminoglycans and related proteoglycans in intrinsically aged human skin in vivo. *Exp Dermatol*. 2011;20(5):454–456.
20. Ghatak S, Maytin EV, Mack JA, et al. Roles of proteoglycans and glycosaminoglycans in wound healing and fibrosis. *Int J Cell Biol*. 2015;2015:834893.
21. Schmittgen TD, Livak KJ. Analyzing real-time PCR data by the comparative C(T) method. *Nat Protoc*. 2008;3(6):1101–1108.
22. Bei Y, Wang F, Yang C, Xiao J. Telocytes in regenerative medicine. *J Cell Mol Med*. 2015;19(7):1441–1454.
23. Dobrev HP. A study of human skin mechanical properties by means of Cutometer. *Folia Med (Plovdiv)*. 2002;44(3):5–10.
24. Dobrev HP. In vivo study of skin mechanical properties in patients with systemic sclerosis. *J Am Acad Dermatol*. 1999;40(3):436–442.
25. Prydz K, Dalen KT. Synthesis and sorting of proteoglycans. *J Cell Sci*. 2000;113(pt 2):193–205.
26. Nadanaka S, Zhou S, Kagiya S, et al. EXTL2, a member of the EXT family of tumor suppressors, controls glycosaminoglycan biosynthesis in a xylose kinase-dependent manner. *J Biol Chem*. 2013;288(13):9321–9333.
27. Beaty NB, Mello RJ. Extracellular mammalian polysaccharides: glycosaminoglycans and proteoglycans. *J Chromatogr*. 1987;418:187–222.
28. Cateson B, Christner JE, Baker JR, Couchman JR. Production and characterization of monoclonal antibodies directed against connective tissue proteoglycans. *Fed Proc*. 1985;44(2):386–393.
29. Mlosek RK, Malinowska S. Ultrasound image of the skin, apparatus and imaging basics. *J Ultrason*. 2013;13(53):212–221.
30. Lavker RM, Zheng PS, Dong G. Aged skin: a study by light, transmission electron, and scanning electron microscopy. *J Invest Dermatol*. 1987;88(3 suppl):44s–51s.
31. Kamma-Lorger CS, Pinali C, Martinez JC, et al. Role of decorin core protein in collagen organisation in congenital stromal corneal dystrophy (CSCD). *PLoS One*. 2016;11(2):e0147948.
32. Li Y, Xia W, Liu Y, Remmer HA, Voorhees J, Fisher GJ. Solar ultraviolet irradiation induces decorin degradation in human skin likely via neutrophil elastase. *PLoS One*. 2013;8(8):e72563.
33. Li Y, Liu Y, Xia W, Lei D, Voorhees JJ, Fisher GJ. Age-dependent alterations of decorin glycosaminoglycans in human skin. *Sci Rep*. 2013;3:2422.
34. Nomura Y. Structural change in decorin with skin aging. *Connect Tissue Res*. 2006;47(5):249–255.
35. Lochner K, Gaemlich A, Südel KM, et al. Expression of decorin and collagens I and III in different layers of human skin in vivo: a laser capture microdissection study. *Biogerontology*. 2007;8(3):269–282.
36. Lapiere CM, Nusgens BV. [The extracellular matrix and its regulation]. *Pathol Biol (Paris)*. 1992;40(2):133–138.
37. Daly CH. Biomechanical properties of dermis. *J Invest Dermatol*. 1982;79(suppl 1):17s–20s.
38. Lewis JL, Krawczak DA, Oegema TR Jr, Westendorf JJ. Effect of decorin and dermatan sulfate on the mechanical properties of a neocartilage. *Connect Tissue Res*. 2010;51(2):159–170.
39. Wan D, Small KH, Barton FE. Face lift. *Plast Reconstr Surg*. 2015;136(5):676e–689e.
40. Werschler WP, Werschler PS. Long-term efficacy of micro-focused ultrasound with visualization for lifting and tightening lax facial and neck skin using a customized vectoring treatment method. *J Clin Aesthet Dermatol*. 2016;9(2):27–33.
41. Lee IH, Nam SM, Park ES, Kim YB. Evaluation of micro-focused ultrasound for lifting and tightening the face. *Arch Aesthetic Plast Surg*. 2015;21(2):65.
42. Fabi SG. Noninvasive skin tightening: focus on new ultrasound techniques. *Clin Cosmet Investig Dermatol*. 2015;8:47–52.
43. Harris MO, Sundaram HA. Safety of microfocused ultrasound with visualization in patients with Fitzpatrick skin phototypes III to VI. *JAMA Facial Plast Surg*. 2015;17(5):355–357.
44. Rusu MC, Mirancea N, Mănoiu VS, Vălcu M, Nicolescu MI, Păduraru D. Skin telocytes. *Ann Anat*. 2012;194(4):359–367.
45. Ceafalan L, Gherghiceanu M, Popescu LM, Simionescu O. Telocytes in human skin – are they involved in skin regeneration? *J Cell Mol Med*. 2012;16(7):1405–1420.
46. Manetti M, Guiducci S, Ruffo M, et al. Evidence for progressive reduction and loss of telocytes in the dermal cellular network of systemic sclerosis. *J Cell Mol Med*. 2013;17(4):482–496.
47. Reed CC, Iozzo RV. The role of decorin in collagen fibrillogenesis and skin homeostasis. *Glycoconj J*. 2002;19(4–5):249–255.

Clinical, Cosmetic and Investigational Dermatology

Publish your work in this journal

Clinical, Cosmetic and Investigational Dermatology is an international, peer-reviewed, open access, online journal that focuses on the latest clinical and experimental research in all aspects of skin disease and cosmetic interventions. This journal is included on PubMed. The manuscript management system is completely online

Submit your manuscript here: <https://www.dovepress.com/clinical-cosmetic-and-investigational-dermatology-journal>

Dovepress

and includes a very quick and fair peer-review system, which is all easy to use. Visit <http://www.dovepress.com/testimonials.php> to read real quotes from published authors